

# COOLING ROOFS THROUGH LOW TEMPERATURE SOLAR-HEAT TRANSFORMATIONS IN HYDROPHILIC POROUS MATERIALS

D. Karamanis<sup>\*1</sup>, E. Vardoulakis<sup>1</sup>, E. Kyritsi<sup>1</sup>, V. Kapsalis<sup>1</sup>, G. Gorgolis<sup>1</sup>, S. Krimpalis<sup>1</sup>, G. Mihalakakou<sup>1</sup>, N. Ökte<sup>2</sup>

*1 Department of Environmental & Natural Resources Management, University of Patras  
Seferi 2, 30100  
Greece*

*2 Department of Chemistry, Boğaziçi University,  
Bebek 34342, Istanbul, Turkey*

*\*Corresponding author: dkaraman@cc.uoi.gr*

## ABSTRACT

The principle of roofs cooling through the water vapour adsorption-desorption cycle in porous materials is presented. In order to study the effect, porous materials of natural origin or synthesized at our lab, were characterized at the micro-scale with SEM, XRD, UV-VIS-NIR spectrometry, thermal and water-vapour adsorption measurements and tested at the urban scale in a wind tunnel of controlled environmental conditions and simulated sun. In the later, the difference of temperature increase under simulated solar irradiation (300 W/m<sup>2</sup>) between a highly hydrophilic mesoporous sample and marble dust with comparable reflectance was almost 5 °C in the first irradiation hours and reduced to 2 °C at the end of irradiation.

## KEYWORDS

Solar cooling, hydrophilic materials, solar-heat transformation, solar multifunctional nanocomposites

## 1 INTRODUCTION

Rapid urbanization and economic development in many countries during the last century resulted in microclimate changes of cities, mainly due to man-made constructions. High temperatures appear during the summer and form a serious societal problem (Santamouris, 2013). For example, the mean temperature in Tokyo during the last 100 years has been raised 3 to 4 °C, while there has been an increase to the number of the nights in which the temperature in Tokyo is over 25 °C, from 10 to 40 during the last decade (Okada et al., 2008). In Athens, temperature differences between urban and suburban stations up to 10 °C have been observed (Santamouris et al., 1999). Even in smaller cities in Greece, the temperature differences between the urban and rural areas seem to be high (Kolokotsa et al., 2009; Vardoulakis et al., 2013). This temperature increase due to the urban heat island phenomenon can be quantified by measuring the maximum temperature difference between urban and suburban areas which is specified as heat island intensity.

Consequences of this phenomenon are energy consumption increase due to air-conditioning, thermal discomfort inside the city environment, growth in peak energy demand and money loss (Akbari et al., 1997, Nikolaidis et al., 2009), even heat related deaths in some cases (Johnson and Wilson, 2009). The accumulation of heat inside the urban spar is clearly involved with the urban design and structure density of building in cities. Heat island effect is mainly caused by the reduction of wind speed, due to the high rise building development, which results in low convective heat removal. Moreover, the reduction of permeability of the ground and the usage of materials that absorb and store solar radiation increase the heat

capacity of the cities and diminish the cooling effect of evaporation. Due to the lack of green areas, it was reported that evapotranspiration in Tokyo has been reduced by 38% from 1972 to 1995 (Kondoh et al., 2000). Additionally, an important factor for the heat island appearance is waste heat generated from low energy efficient devices, factories and automobiles, the anthropogenic heat.

Much research was carried out to solve the problem and reduce the energy consumption in buildings. Proposals like the reduction of anthropogenic heat and the proper urban design were recommended. Constraining this problem requires a combination of countermeasures since presented techniques so far have advantages and disadvantages. Increasing the area of green tract land or the surface area of water (eg. artificial lakes and ponds) prevent the heat island phenomenon. However, the high land value of urban space limits the wide applicability of these methods. On the contrary, roofs provide an excellent space to apply mitigation techniques and save buildings' energy consumption (Santamouris, 2012). Roof surfaces are a key element of the heat exchange in city environment, since they take up a great percentage of urban area (up to 20%) and are exposed to solar radiation for many hours every day. For arid areas, almost 50% of the heat load in the building comes from the roof (Nahar et al., 1997), so it is of great importance to understand and reduce the heat movement and storage during a daytime cycle, due to radiation, conduction and convection at roof surface (Meyn et al., 2009). In this direction, the most important mitigation technologies are cool or reflective roofs and green roofs (Santamouris, 2012). Both technologies can lower the surface temperatures of roofs and thus decrease the corresponding sensible heat flux to the atmosphere. However, there are important considerations for both technologies. For example, reflective coatings over roof reduce cooling loads by 18 to 93% (Synnefa et al., 2007) but their reflectivity reduces even 15% during the first year of the application due to weathering (Bretz et al., 1997). Although the cost of green roofs has been highly reduced, the need of water for the irrigation and drainage systems as well as the required intensive maintenance and the dependence on the local climate conditions can limit their worldwide applicability. Therefore, new and more efficient materials and procedures have to be developed (Santamouris, 2012).

Evaporative cooling is a well known and efficient technique in passive cooling (Alvarado et al., 2009) and many methods have been studied by applying a thin film of water over the roof (Sanjay et al., 2008) or by using phase change materials for heating and cooling the building (Pasupathy et al., 2007). During the last years, intensive research about evaporative cooling has been developed and mainly concentrated on the use of natural porous materials for roof-surface treatment (Meng et al., 2005, Okada et al., 2009, Wanphen et al., 2009). According to the evaporative cooling principle, rainwater or humidity adsorbed from porous materials during rainfall or during high humidity nights, can be stored inside small pores and channels in a porous material. Reversely, during a sunny day, humidity stored inside the pores, is released and maintains roof surface temperature at low levels due to latent heat of water evaporation. Lowering the roof surface temperature is important, since heat transfer inside the building reduces as well. Also, there are many indirect benefits like water retention during a heavy rainfall, increase of thermal insulation of the building and removal of many polluting elements. Moreover, roof material degradation due to high roof temperatures is reduced, while relative humidity in winter changes environmental climate to more wet states, resulting in reduction of diseases spread like influenza (Okada et al., 2008).

In order to choose the appropriate material for applications of evaporative cooling, a set of properties must be satisfied:

- Ability to absorb water or vapour at different relative pressure
- High water retention
- Thermal, hydrothermal and ageing stability
- Being locally available and inexpensive
- Environmentally non toxic and easily to handle
- Easy construction into required shape and size for roof application
- Added ability for CO<sub>2</sub> and toxic pollutants sorption
- Easy scale-up production

The principle of building integrated evaporative cooling has been validated with the addition of liquid water in natural porous materials and irradiation from a metal halide lamp ( $500 \text{ W/m}^2$ ) (Wanphen et al., 2009), synthetic and aluminum pillared clays (Vardoulakis et al., 2011) or modified lignite fly ash (Karamanis et al., 2012) with metal halide lamp ( $\sim 100 \text{ W/m}^2$ ) and pHEMA polymer and sun simulation of class A, AM1.5 (Rotzetter et al., 2012). Recently, we showed that the principle can be applied by moisture sorption on the highly hydrophilic natural sepiolite (Karamanis et al., 2012). With overnight uptake of water vapor on porous sepiolite in 70% relative humidity (to resemble the night outdoor condition), lower surface temperatures were observed under low simulated solar irradiation in comparison to concrete due to heat absorption for water evaporation and desorption with the accompanied mass reduction. Sepiolite, a fibrous magnesian silicate made up of talk-like layers arranged in long ribbons stuck together to form the fibers, adsorbs water vapor on the external surfaces, in microporous channels and inter-fiber micropores and in larger pores that are also present between fibers (Karamanis et al., 2012). In addition, we have seen that by in situ buildup of  $\text{TiO}_2$  in sepiolite (Karamanis et al., 2012) or  $\text{ZnO}$  nanoparticles on the surface of fly ash cenospheres (Ökte et al., 2013), the water vapour adsorption capacity of the porous matrix is retained while the photoresponsive can be used for pollutants photocatalytic degradation. This simultaneous multifunction is possible since different parts of the solar spectrum are being utilized, ie. UV-VIS for photodegradation and VIS-IR for providing the thermal energy for phase changes. *Obviously, the design of appropriate materials for roof covering with combined properties of high reflectance (especially in the visible range), moisture sorption and evaporation through infrared absorbance and self cleaning through ultraviolet absorbance could contribute significantly to the reduction of the heat flux entering the building from the roof.*

In the selection of the hydrophilic porous matrix, it is customary to distinguish between water vapor adsorption in the micropores of porous materials (pore widths of less than 2 nm) and mesopores (2-50 nm). In the former, micropore filling (and cooperative filling) is the dominant mechanism. Recent investigations in low-temperature solar energy storage applications with water sorption on microporous aluminophosphates have shown that the driving force for the water sorption process is the formation of highly ordered water clusters in the micropores (Ristic et al., 2012). Due to the strong water confinement, temperatures of up to  $140^\circ \text{C}$  are needed for water desorption and these can be reached by solar thermal collectors (e.g., evacuated tube collectors). In the mesoporous materials, the exothermic process of capillary condensation is observed (preceded by a molecular layering on the pore walls) with the appearance of a dense liquid-like state in mesoporous adsorbents for chemical potential lower than its bulk saturating value. In cylindrical mesopores, the adsorbant is confined in two dimensions, the confinement effects are greater and capillary condensation is observed at lower pressures. A similar phenomenon occurs on desorption, with the system persisting in the liquid state at chemical potentials (pressures) below the true equilibrium value. Therefore, the principle of solar cooling with the mesoporous materials can be extended to account for all the phase changes within the adsorption-condensation-evaporation-desorption cycle as: after overnight water vapor adsorption and capillary condensation, liquid water in the mesopores will be desorbed in lower temperatures than the bulk liquids due to solar radiation absorption for providing the sensible and latent heats as well as the heat of desorption. In this way, the temperature of the mesoporous material surface should be highly reduced after these low-temperature solar-heat transformations.

In this work, we studied the interaction of solar irradiation with porous materials of natural origin or synthetic (purchased or prepared) in comparison to PCMs and materials used in the external building surfaces. The interaction was studied with UV-VIS-NIR reflectance-absorbance spectroscopy as a function of the incident wavelength (200-2500 nm) and in a wind tunnel of adjustable environmental parameters as mass and temperature variation under simulated radiation. Prior to the interaction experiments, all materials were characterized with different techniques while their thermal and optical properties were also determined.

## 2 EXPERIMENTAL

A mesoporous material was prepared and characterized with techniques like X-ray diffraction (XRD) and nitrogen adsorption–desorption isotherms. Since  $\text{TiO}_2$  is a well known photoresponsive material with self-cleaning properties and in order to test the variability of the porous matrix in water vapour adsorption,  $\text{TiO}_2$  nanoparticles were in situ prepared in the mesoporous sample through the sol-gel method with low Ti concentration (7 wt% as deduced from SEM-EDX measurements). Their surface morphology was determined by scanning electron microscopy with energy-dispersive X-ray spectroscopy (SEM-EDX). The thermogravimetry (TG) and differential thermogravimetry (DTG) measurements was performed on a STA 449C (Netzsch-Gerätebau, GmbH, Germany) thermal analyzer. The heating range was from ambient temperature up to 150 °C, with a heating rate of 2 °C min<sup>-1</sup> under synthetic air flow. Prior to measurements, the samples were put in desiccators of specific relative humidity. The optical characterization of the samples with pre-determined adsorbed water vapor was conducted by a UV/VIS/NIR spectrophotometer (Lambda 950 of PerkinElmer fitted with a 150 mm diameter InGaAs integrating sphere that collects both specular and diffuse radiation) over the solar spectrum (200–2500 nm). The equipment was calibrated with a set of Labsphere certified standards while the ASTM G173-03 reference spectrum was used to normalize the data. Thermal conductivity of the samples was measured by a KD2 Pro meter (Decagon Devices) using the transient line heat source method while infrared emittance was recorded with a high resolution thermographic camera (VarioCAM). Water adsorption capacity of the produced materials was examined as a function of relative humidity and time. In the moisture sorption isotherms, samples were placed in desiccators with saturated salt solutions for controlling relative humidity while temperature was air-conditionally controlled at 25°C. Prior to measurements, samples were dried to constant mass in an air-circulated oven at 105°C. In order to determine the sorption isotherms, the samples were periodically weighed and the moisture content was calculated as the difference of mass measurements in different time periods and the initial dry state.

The water sorption properties and the associated surface temperature reduction were conducted in an in-house designed and built wind tunnel of controllable conditions of air relative humidity, temperature and wind flow (Vardoulakis et al., 2011). The wind tunnel consists of five parts: the setting entrance, the contraction zone, the diffuser, the test section and the fan housing. Wind flow (m<sup>3</sup> h<sup>-1</sup>), relative humidity (%) and temperature (°C) of air inside the tunnel, the weight of the sample and the temperatures of the T-type thermocouples at the surface and middle layers of the sample cell are recorded by a CR1000 data logger (Campbell Scientific). The solar radiation can be simulated with a metal halide lamp or two 80 W Philips xenon lamps or a recently acquired 1 sun solar simulator (LOT-ORIEL). The reflected radiation and the power stability of the lamps are monitored by an inverted ISO second-class pyranometer on the top of the test section of the tunnel. The incoming radiation at the test cell position (typical 6x6x3 cm<sup>3</sup> but several volumes are available) is measured with a portable digital solar meter. Every material test is lasted at least for 48 h. In the morning the lamp is turned on for a period of 12 h and the cycle is repeated for one more day. The relative humidity is raised to 70% at night with lamp off. In this work, typical soil (used in green roofs) and marble dust (calcium carbonate) were also tested for comparison purposes.

## 3 RESULTS & DISCUSSION

The materials' morphology was of mesoporous structure with pore diameter in the corresponding region. In Fig. 1, the absorption spectra of the MESO sample after the adsorption of water vapor at different humidity, are shown. In the same figure, the spectra of

the MESO sample and the TiO<sub>2</sub>-MESO composite as stored in room conditions are also included. In the NIR region of the spectrum for the MESO sample saturated at 75% relative humidity (RH), four main maxima located at c. 970 nm, c. 1190 nm, c. 1450 nm and c. 1930 nm are clearly observed, indicating the water vapor condensation within the mesopores. These maxima correspond to the second overtone of the OH stretching band ( $3\nu_{1,3}$ ), the combination of the first overtone of the O–H stretching and the OH-bending band ( $2\nu_{1,3} + \nu_2$ ), first overtone of the OH-stretching band ( $2\nu_{1,3}$ ) and combination of the OH-stretching band and the O-H bending band ( $2\nu_{1,3} + \nu_2$ ), respectively. In the MESO sample saturated at 33% of RH, the intensity of the maxima is much lower due to the reduction of the adsorbed water vapor. By normalizing the absorption data with the solar spectral irradiance ASTM G-173, an increase of the NIR to TOTAL absorption ratio from 31% to 42% was calculated for the two samples at 33% and 93% RH, respectively. The same peaks are also observed for the pure MESO and the TiO<sub>2</sub>-MESO composite (Fig 1). Since room RH varies between 40-60%, the peaks intensity of the room stored samples is within the respective of the samples at 33% and 75% of RH. The buildup of the TiO<sub>2</sub> nanoparticles on the MESO surfaces retained the IR spectrum, increased the reflectance in the VIS due to white titania and the absorbance in the UV due to the TiO<sub>2</sub> photocatalytic action under UV light. Therefore, the TiO<sub>2</sub>-MESO composite improved its optical properties towards its utilization in multifunctional applications. The absorption spectra of marble dust (CaCO<sub>3</sub>) that is used as external building surface, is also shown in Fig. 1. The marble dust shows the highest reflectance of all the studied materials, indicating its suitability as a “cool” reflective material. In addition, the intense 1412 nm peak in the CaCO<sub>3</sub> spectrum as well as others of lower intensity, are mainly due to water bound in the structure since are observed in both dried and room stored samples.

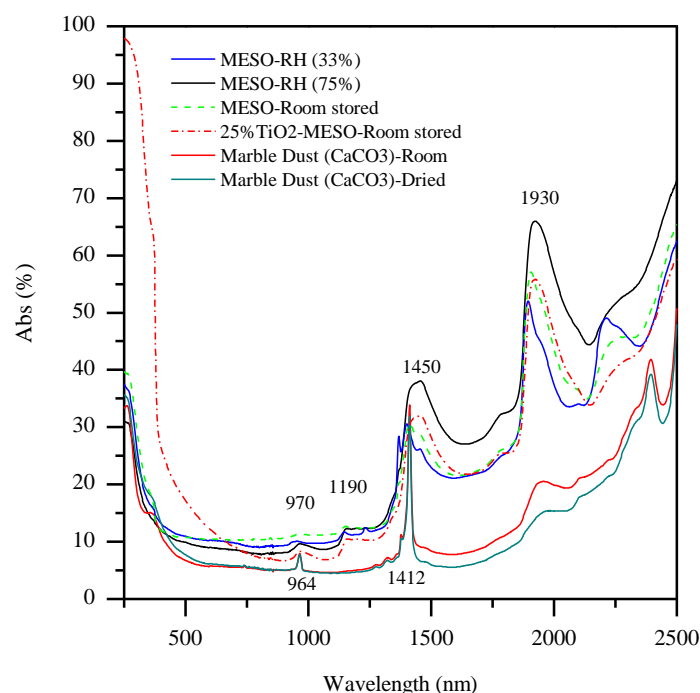


Figure 1. Absorbance spectra of the MESO and 25%TiO<sub>2</sub>-MESO materials as room stored, MESO after water vapor adsorption 33% and 75% of RH and marble dust (CaCO<sub>3</sub>) as received (room stored) and after drying.

According to the thermogravimetric results of Fig. 2, there is one major endothermic peak of temperature around 55 °C where the physisorbed and condensed water is released from the mesoporous material. This “free water” bound due to condensation is being removed by the low temperature heating fluxes through evaporation and desorption from the pores. In contrast, water molecules bound to materials like zeolites through the adsorption bonds of physical adsorption demand higher heats of desorption but also higher temperatures for their removal

from materials' pores. In the proposed application of materials integration in building surfaces, the temperature rise of an absorbing building surface with 0.05 reflectance can be about 34 -50 °C warmer than the ambient air in full sunlight. Therefore, the mesostructured samples are appropriate for such applications and almost all of the sorbed water is expected to be removed under the summer solar radiation. Furthermore, the thermal conductivity of the MESO material at room conditions was measured 0.16 W m<sup>-1</sup> K<sup>-1</sup> and was reduced to 0.099 W m<sup>-1</sup> K<sup>-1</sup> after drying the sample at 200 °C for 2 h.

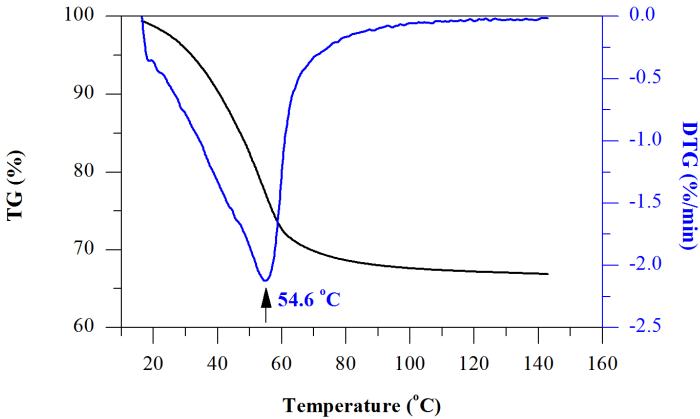


Figure 2. TG and DTG curves of the MESO material after water vapor adsorption at 75% RH.

The hydrophilicity of the MESO samples and the supported TiO<sub>2</sub> nanocatalyst was investigated by the water vapor adsorption isotherms. Fig. 3 shows the water vapor sorption isotherm of the tested materials at 25 °C. For comparison purposes, soil, marble dust (CaCO<sub>3</sub>) and silica gel isotherm curves are also included. Water vapor sorption in soil and marble dust was very low in the whole scale of relative pressures. The isotherms of silica gel and MESO samples showed different type behaviour. The silica sorption isotherm was of type I in the IUPAC classification indicating a highly hydrophilic material with water vapor sorption ability up to 0.25 g g<sup>-1</sup>.

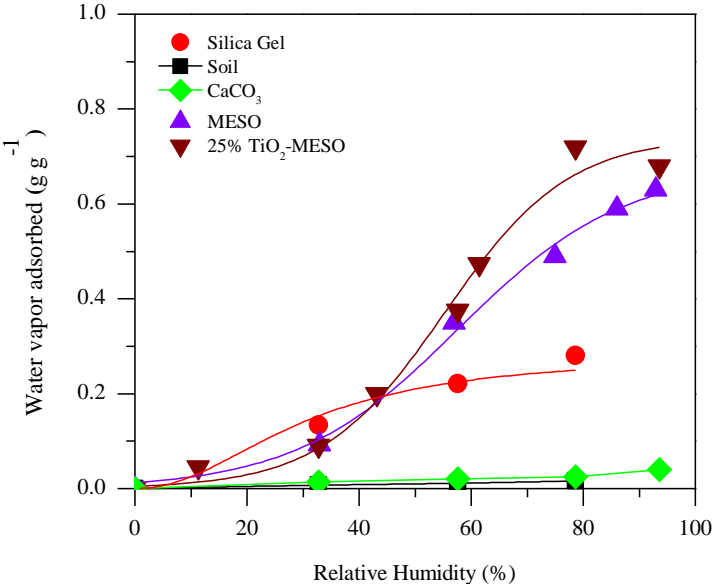


Figure 3: Water vapor adsorption isotherms on the MESO samples, TiO<sub>2</sub>-MESO, soil, silica gel and CaCO<sub>3</sub> at 25 °C.

In contrast, the water adsorption isotherm on the MESO samples was of type V. This is indicative of a relatively hydrophobic character in the low-pressure region of the adsorption

isotherm but with a capillary condensation step 0.55-0.6 relative pressure leading to a total filling of the pore volume and thus to a type-V isotherm (with maximum uptake more than 0.6 g g<sup>-1</sup> at 93 % RH). Upon TiO<sub>2</sub> in situ buildup on the MESO sample, the hydrophilicity of the composite was maintained and the catalyst still exhibited a type V isotherm (Fig. 3).

The MESO material was further tested in the wind tunnel under simulated solar irradiation in comparison to soil and marble dust. The radiation was provided by two low power xenon lamps over the top of the wind tunnel. The incoming radiation at the test cell position was measured at several points of the cell with an average of 300 W m<sup>-2</sup>. Every material test lasted at least for 48 h. In the morning, the lamp was turned on for a period of 12 h and the cycle was repeated for one more day. The relative humidity was raised to 70% at night with lamp off. The weight variation curve of the samples revealed that the soil and marble masses remained almost constant at night with increased RH while the MESO mass increased more than 15 % within the 12 hours period. Upon irradiation its mass decreased almost exponentially due to the evaporation and desorption of night sorbed water.

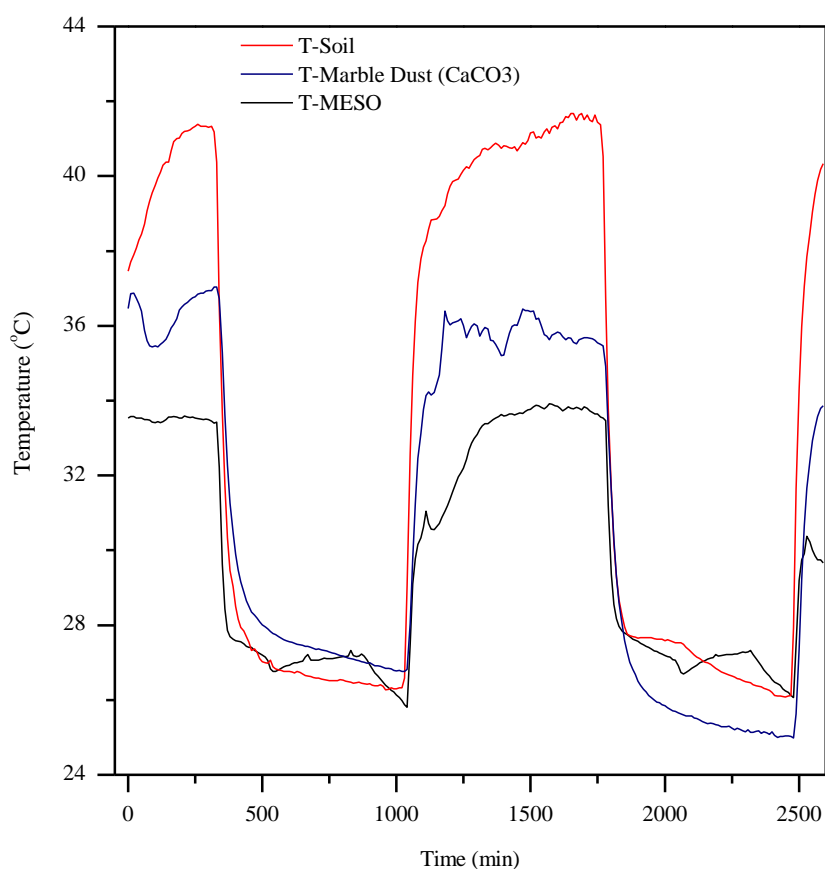


Figure 4: Temperature increase inside the MESO, soil and CaCO<sub>3</sub> samples due to low simulated solar irradiation (average 300 W m<sup>-2</sup>).

Fig. 4 shows the measured temperature increase in the cyclic experiments with simulated solar radiation of two continuous cycles, starting from the first lamp on as the zero time. The difference of temperature increase under simulated solar irradiation between the MESO sample and marble dust with comparable reflectance was almost 5 °C in the first irradiation hours and reduced to 2 °C at the end of irradiation. The MESO difference with the soil sample was even higher. By considering a latent heat of 2300 kJ kg<sup>-1</sup> for water vaporization at the attained material temperatures, the observed MESO mass reduction of 1 g (13% of the initial mass) corresponds to 2.3 kJ of absorbed energy for water evaporation or half of the absorbed incoming radiation. The evaporation term was absent in CaCO<sub>3</sub> that exhibits comparable

reflectance to MESO and very small in soil with the very low reflectance. These results indicate the material's suitability for the proposed application of evaporative cooling.

#### 4 CONCLUSIONS

Key factor in reducing energy consumption in buildings is the materials used in the building sector. In order to sustain our natural resources through the utilization of the abundant solar energy, new cooling principles should be applied and, if possible, be integrated in the building from the manufacturing phase. In this work, the solar-heat transformation for the evaporation of night adsorbed and condensed water vapor in novel highly hydrophilic mesoporous materials of high reflectance has been found to contribute significantly in the temperature reduction of the irradiated surface and consequently, the heat flux transferred through the surface. Although some direct applications of the hydrophilic materials could be investigated like the cooling effect of materials' addition in green roofs, further combined research and development is needed for their technological implementation and building integration.

#### 5 ACKNOWLEDGEMENTS

This work has been supported by the University of Western Greece, Latsis Foundation and GSRT programmes of Hrakleitos II, Greece-Turkey Bilateral Program and ARISTEIA I ("Operational Programme Education and Lifelong Learning co-funded by the European Social Fund (ESF) and National Resources). Thanks are due to the Horizontal Network of Laboratories of the University of Ioannina and Bogazici University for the help in materials' characterization.

#### 6 REFERENCES

- Akbari, H., Bretz, S., Kurn, D. and Hanford, J. (1997). Peak power and cooling energy savings of high-albedo roofs. *Energy and Buildings* 25 (2), 117- 126.
- Alvarado, J., Terrell, W. and Johnson, M. (1999). Passive cooling systems for cement-based roofs. *Building and Environment*, 44 (9), 1869-1875.
- Bretz, S. and Akbari, H. (1997). Long-term performance of high-albedo roof coatings. *Energy and Buildings*, 25 (2), 159-167.
- Johnson, D.P. and Wilson, J.S. (2009). The socio-spatial dynamics of extreme urban heat events: The case of heat-related deaths in Philadelphia. *Applied Geography*, 29, 419-434.
- Karamanis, D., Vardoulakis, E. (2012) Application of zeolitic materials prepared from fly ash to water vapor adsorption for solar cooling. *Applied Energy*, 97, 334-339.
- Karamanis, D., Vardoulakis, E., Kyritsi, E., Ökte, N. (2012). Surface solar cooling through water vapor desorption from photo-responsive sepiolite nanocomposites. *Energy Conversion and Management*, 63, 118-122.
- Kolokotsa, D., Psomas, A. and Karapidakis E., (2009). Urban heat island in southern Europe: The case study of Hania, Crete. *Solar Energy*, 83 (10) 1871-1883.
- Kondoh, A. and Nishiyama, J. (2000). Changes in hydrological cycle due to urbanization in the suburb of Tokyo Metropolitan area, Japan. *Advances in Space Research*, 26 (7), 1173-1176.



- Meng, Q, Hu, W. (2005). Roof cooling effect with humid porous medium. *Energy and Buildings*, 37, 1-9
- Meyn, S. and Oke, T. (2009). Heat fluxes through roofs and their relevance to estimates of urban heat storage. *Energy and buildings* 41, 745-752.
- Nahar, N.M., Sharma, P. and Purohit, M.M. (1997). Studies on solar passive cooling techniques for arid areas. *Energy Conversion & Management*, 40, 89-95.
- Nikolaidis, Y., Pilavachi, P. and Chletsis, A. (2009). Economic evaluation of energy saving measures in a common type of Greek building. *Applied Energy*, 86 (12), 2550-2559.
- Okada, K., Matsui, S., Isobe, T., Kameshima, Y. and Nakajima, A. (2008). Water-retention properties of porous ceramics prepared from mixtures of allophone and vermiculite for materials to counteract heat island effects. *Ceramics International*, 34 (2), 345-350.
- Okada, K., Ooyama, A., Isobe, T., Kameshima, Y, Nakajima, A. and MacKenzie, K. (2009). Water retention properties of porous geopolymers for use in cooling applications. *Journal of the European Society*, 29, 1917-1923.
- Ökte, N., Karamanis, D. A novel photoresponsive ZnO-flyash nanocomposite for environmental and energy applications. (2013) *Applied Catalysis B: Environmental*, 142-143, 538-552.
- Pasupathy, A. and Velraj, R. (2007). Effect of double layer phase change material in building roof for round thermal management. *Energy and Building*, 40, 193-203.
- Ristic, A., Logar, N., Henninger, S., Kaucic, V. (2012) The performance of small-pore microporous aluminophosphates in low-temperature solar energy storage: the structure–property relationship. *Advanced Functional Materials*, 22, 1952-1957.
- Rotzetter, A.C.C., Schumacher, C.M., Bubenhofer, S.B., Grass, R.N., Gerber, L.C., Zeltner, M., Stark, W.J. (2012). Thermoresponsive polymer induced sweating surfaces as an efficient way to passively cool buildings. *Advanced Materials*, 24, 5352–5356.
- Sanjay, J., and Chand, P. (2008). Passive cooling techniques of buildings: Past and present- A review, *Engineering Energy*, 4, 37-46
- Santamouris, M., Michalakakou, G., Papanikolaou, N. and Assimakopoulos, DN (1999). A neural network approach for modelling the heat island phenomenon in urban areas during the summer period. *Geophysical Research Letters*, 26 (3), 337-340.
- Santamouris, M. (2012). Cooling the cities – A review of reflective and green roof mitigation technologies to fight heat island and improve comfort in urban environments. *Solar Energy*, (in press).
- Santamouris, M. (2013). Using cool pavements as a mitigation strategy to fight urban heat island—A review of the actual developments. *Renewable Sustainable Energy Reviews*, 26, 224-240.
- Synnefa, A., Santamouris, M. and Akbari, H. (2007). Estimating the effect of using cool coatings on energy loads and thermal comfort in residential buildings in various climatic conditions. *Energy and Buildings* 39 (11), 1167-1174.
- Vardoulakis, E., Karamanis, D., Fotiadi, A., Mihalakakou, G. (2013). The urban heat island effect in a small Mediterranean city of high summer temperatures and cooling energy demands. *Solar Energy*, 94, 128-144.

- Vardoulakis, E., Karamanis, D., Mihalakakou, G., Assimakopoulos, M.N. (2011). Solar cooling with aluminium pillared clays. *Solar Energy Materials and Solar Cells*, 95, 2363–70.
- Wanphen S. and Nagano K. (2009) “Experimental study of the performance of porous materials to moderate the roof surface temperature by its evaporative cooling effect”, *Building and Environment* **44** pp338-351.